Mean flow instabilities of two-dimensional convection in strong magnetic fields

By A.M. RUCKLIDGE[1]†, M.R.E. PROCTOR[2], and J. PRAT[3]

[1] Department of Applied Mathematics, University of Leeds, Leeds, LS2 9JT, UK

[2] Department of Applied Mathematics and Theoretical Physics, University of Cambridge, Cambridge, CB3 0WA, UK

[3] Departament de Matemàtica Aplicada IV, Universitat Politècnica de Catalunya (EPSEVG), 08800 Vilanova, Spain

(Received 3 January 2006)

The interaction of magnetic fields with convection is of great importance in astrophysics. Two well-known aspects of the interaction are the tendency of convection cells to become narrow in the perpendicular direction when the imposed field is strong, and the occurrence of streaming instabilities involving horizontal shears. Previous studies have found that the latter instability mechanism operates only when the cells are narrow, and so we investigate the occurrence of the streaming instability for large imposed fields, when the cells are naturally narrow near onset. The basic cellular solution can be treated in the asymptotic limit as a nonlinear eigenvalue problem. In the limit of large imposed field the instability occurs for asymptotically small Prandtl number. The determination of the stability boundary turns out to be surprisingly complicated. At leading order, the linear stability problem is the linearisation of the same nonlinear eigenvalue problem, and as a result, it is necessary to go to higher order to obtain a stability criterion. We establish that the flow can only be unstable to a horizontal mean flow if the Prandtl number is smaller than order $B_0^{-4/3}$, where B_0 is the imposed magnetic field, and that the mean flow is concentrated in a horizontal jet of width $B_0^{-1/6}$ in the middle of the layer. The result applies to stress-free or no-slip boundary conditions at the top and bottom of the layer.

1. Introduction

The effect of imposed magnetic fields on thermal convection in a conducting fluid has been a subject of active research for many years. The first linear investigations were carried out by Thompson (1951) and Chandrasekhar (1952). For a full description of the linear stability problem, see Chandrasekhar (1961). Since then there have been two main

† Corresponding author. E-mail: A.M.Rucklidge@leeds.ac.uk

strands of research: one motivated by the effects of large scale magnetic fields on the Sun and other stars, and the other by experiments on liquid metals. The subject has been reviewed by Proctor & Weiss (1982) and by Proctor (2004).

The present paper considers the effects of very strong imposed fields. It is well known that the effects of a powerful Lorentz force are to inhibit motions that tend to bend the field lines, as will be described in the next section. When convection takes place in a horizontal layer with strong vertical field, the onset of motion is in tall columns, whose aspect ratio scales as $B_0^{-1/3}$, where B_0 is a measure of the imposed field. This small aspect ratio enables us to obtain reduced equations for cellular convection. These use the aspect ratio as the small parameter, rather than the usual amplitude expansion, and can therefore be considered fully nonlinear. There have been many investigations of the large B_0 problem, which is in some ways analogous to the situation of the onset of convection in a rapidly rotating layer, for which the aspect ratio is similarly small at onset. Examples of such asymptotic studies are Soward (1974), Bassom & Zhang (1994), Julien & Knobloch (1997,1998,1999) (all in a plane layer) and Abdulrahman *et al.* (2000) (rapidly rotating annulus). Dawes (2001) has combined strong rotation with low Prandtl number (ratio of viscosity to thermal conductivity) to achieve further reductions. Related studies of vortices in ferrofluids have been performed by Russell, Blennerhassett & Stiles (1999). The strong magnetic field problem was first investigated by Proctor (1986), and subsequently by Matthews (1999), and Julien *et al.* (1999, 2000), and Halford & Proctor (2002). Holyer & Proctor (1986) performed an equivalent (though less rigorous) analysis of salt fingers.

A disadvantage of almost all these studies is that the *planform* of the convection is not determined at leading order. Our problem suffers from a similar drawback. However guided by the weakly nonlinear results of Clune & Knobloch (1994), and the computations of Busse & Clever (1996) at moderate B_0 and small Prandtl number, we can be confident that there is a finite range of $\Delta T/\Delta T_c$, (where ΔT is the temperature difference across the layer and ΔT_c its critical value for linear instability) for which two-dimensional solutions are stable. We shall therefore suppose that in our problem for a Boussinesq fluid the preferred planform for convection before the onset of secondary instability takes the form of rolls (independent of one horizontal direction).

It has been known for some time that roll-type solutions can be subject to so-called streaming or shearing instabilities. Willis and Deardorff (1970) reported rolls that oscillated between tilting to the left and tilting to the right. The shearing instability was first discussed in detail by Busse (1972, 1983) and investigated further by Howard & Krishnamurti (1986) and Prat, Massaguer & Mercader (1995) in the non-magnetic case, and for imposed vertical magnetic fields by Matthews *et al.* (1993), Proctor *et al.* (1994) and Rucklidge & Matthews (1996). The three-dimensional problem was considered by Matthews *et al.* (1996). While interesting dynamics of the instability was found, the results were somewhat artificial since the instabilities seemed only to exist for narrow rolls – and not for the wider rolls that would arise naturally at onset (though Rucklidge &

Matthews (1996) report steady and oscillatory shearing behaviour in two-dimensional magnetoconvection at the preferred wavelength).

It is therefore natural to combine the ideas of small-aspect ratio convection in strong fields, and the streaming instability results, to discover under what (if any) circumstances streaming instabilities can occur for cells with a wavelength that arises naturally as the preferred length at onset. In what follows we show that for large magnetic fields and small Prandtl numbers there is a distinguished limit in which the instability occurs and may be identified. Since low Prandtl numbers are characteristic of liquid metals, we are able to make further simplifications based on the large values of the parameter ζ, the ratio of magnetic diffusivity to thermal diffusivity, for such fluids. Low Prandtl number fluid convection is known to be particularly susceptible to secondary instabilities, and has interesting properties even without imposed fields – for example the "flywheel" or "inertial" convection discussed by Proctor (1977) and Busse & Clever (1981), so it is a natural limit to study. It turns out that the study of the onset of the instability within the reduced set of equations is highly non-trivial, and the unstable eigenfunction has a boundary/critical layer structure, in some ways analogous to critical layers in stratified shear flows, though the resolution of the singularity is different in this case. Using boundary layer analysis and accurate numerical simulation we are able to predict and verify the appropriate scalings for the onset of the instability, at least in the limit of large diffusivity ratio ζ. While this is appropriate for laboratory fluids, and the Earth's core, it is not generally applicable to e.g. the solar photosphere. Nonetheless we have done some investigations of the instability in the general case, with ζ of order unity, and find that the high ζ limit gives the correct qualitative picture.

The paper is organised as follows: we describe the governing PDEs for convection in a liquid metal in section 2, and derive asymptotic representations of the convection solution and estimates for the critical parameter values for a mean flow instability in section 3. Numerical results are in section 4, and the paper concludes with a discussion in section 5.

2. Convection in liquid metals

The partial differential equations (PDEs) that describe two-dimensional motion of a fluid heated from below and subjected to a vertical magnetic field are (Proctor & Weiss 1982):

$$\frac{\partial \omega}{\partial t} + \mathrm{J}\left(\Psi, \omega\right) = \sigma \nabla^2 \omega - \sigma R \frac{\partial \theta}{\partial x} - \sigma \zeta Q \left(\frac{\partial \nabla^2 A}{\partial z} + \mathrm{J}\left(A, \nabla^2 A\right) \right), \tag{1}$$

$$\frac{\partial \theta}{\partial t} + \mathrm{J}\left(\Psi, \theta\right) = \nabla^2 \theta + \frac{\partial \Psi}{\partial x}, \tag{2}$$

$$\frac{\partial A}{\partial t} + \mathrm{J}\left(\Psi, A\right) = \zeta \nabla^2 A + \frac{\partial \Psi}{\partial z}, \tag{3}$$

where Ψ is the stream-function, with velocity $\mathbf{u} = \nabla \times (\Psi \hat{\mathbf{y}})$ and y-component of vorticity $\omega = -\nabla^2 \Psi$, θ is the deviation from the static temperature profile so the temperature is $1 - z + \theta$, and A is the deviation from the uniform vertical magnetic field, so the total

magnetic field is $\mathbf{B} = (-\partial A/\partial z, 0, 1 + \partial A/\partial x)$. The horizontal coordinate x and vertical coordinate z are scaled by the height h of the box. Time t is scaled by the thermal diffusion time h^2/κ, where κ is the thermal diffusivity. The viscous Prandtl number $\sigma = \nu/\kappa$ and the magnetic diffusivity ratio $\zeta = \eta/\kappa$ (where ν and η are the viscous and magnetic diffusivities). Temperatures and magnetic fields are scaled by the temperature difference ΔT and the vertical magnetic field $\mathbf{B}_0 = B_0\hat{\mathbf{z}}$ imposed across the box. The other parameters are the Rayleigh number R and the Chandrasekhar number Q:

$$R = \frac{g\alpha h^3}{\kappa\nu}\Delta T, \qquad Q = \frac{h^2}{\mu_0\rho_0\eta\nu}B_0^2, \tag{4}$$

where g is the acceleration due to gravity (acting in the negative z direction), α is the thermal expansion coefficient, ρ_0 is the reference density and μ_0 is the magnetic permeability of the fluid. The nonlinearities, contained in the Jacobian $\mathrm{J}(f,g) = (\partial f/\partial x)(\partial g/\partial z) - (\partial f/\partial z)(\partial g/\partial x)$, represent the transport of vorticity, heat and magnetic flux; in addition, the fluid is driven by the nonlinear Lorentz force.

In liquid metals, magnetic fields diffuse much more effectively than heat does, so the diffusivity ratio $\zeta \gg 1$ (in mercury, for instance, $\zeta \sim 10^5$). We take the limit $\zeta \to \infty$, scaling the flux function A by ζ^{-1} (e.g., Busse & Clever 1996). At leading order in ζ^{-1}, there is a balance between advection and diffusion of the imposed vertical magnetic field:

$$\nabla^2 A \sim -\frac{\partial \Psi}{\partial z} + \mathrm{O}(\zeta^{-1}), \tag{5}$$

and only the linear part of the Lorentz force survives in the momentum equation. The two PDEs of interest are now

$$\frac{\partial \omega}{\partial t} + \mathrm{J}\left(\Psi, \omega\right) = \sigma\nabla^2\omega - \sigma R\frac{\partial \theta}{\partial x} + \sigma Q\frac{\partial^2 \Psi}{\partial z^2}, \tag{6}$$

$$\frac{\partial \theta}{\partial t} + \mathrm{J}\left(\Psi, \theta\right) = \nabla^2\theta + \frac{\partial \Psi}{\partial x}. \tag{7}$$

Note that this simple reduction, which holds independent of the electromagnetic boundary conditions, can only be performed in the 2D case. We consider two sets of idealised boundary conditions, with fixed temperature, no normal velocity and either stress-free or no-slip conditions at the top and bottom of the layer ($z = 0$, 1). These amount to $\theta = \Psi = 0$ at $z = 0$, 1, as well as either $\partial^2\Psi/\partial z^2 = 0$ (stress-free) or $\partial\Psi/\partial z = 0$ (no-slip). We take periodic boundary conditions in the horizontal (x) direction, with wavelength $2\pi/k$.

We emphasize again that taking the limit $\zeta \to \infty$ is not an essential step in our calculations below; it merely serves to simplify the presentation, and avoids the difficulty of a primary oscillatory instability (which requires a small value of ζ).

3. Asymptotics with large magnetic field

As it is the nonlinear part of the Lorentz force that has been removed, the linear stability properties of (1–3) and (6–7) are essentially the same (see Chandrasekhar 1961). With a fixed magnetic field strength Q, the primary instability at $R = R_c$ as the temper-

ature difference across the layer is increased is to steady convection rolls with horizontal wavenumber $k = k_c$, with

$$R_c = \frac{(\pi^2 + k_c^2)^3}{k_c^2} + \frac{\pi^2 + k_c^2}{k_c^2}\pi^2 Q, \quad \text{where } k_c \text{ satisfies} \quad Q = \frac{(\pi^2 + k_c^2)^2(2k_c^2 - \pi^2)}{\pi^4}, \quad (8)$$

assuming stress-free boundary conditions at the top and bottom of the layer. As the imposed field strength Q is increased, the primary instability occurs at

$$R_c \sim \pi^2 Q + \mathrm{O}(Q^{2/3}), \qquad k_c \sim \left(\frac{\pi^4 Q}{2}\right)^{1/6} + \mathrm{O}(Q^{-1/6}). \quad (9)$$

The same asymptotic result holds with stress-free and with no-slip boundary conditions.

Before we begin the stability analysis, we briefly go through the arguments that lead to the nonlinear eigenvalue problem (following Matthews 1999), but with the addition that we are taking the Prandtl number to be small.

3.1. *Nonlinear eigenvalue problem*

In this problem, the small parameter is the horizontal length scale $\delta = 1/k_c$, determined by the large imposed value of Q through (8). We seek steady solutions of the PDEs (6–7), scaling x by δ. We also define $r = R/R_c$, where Q and R_c are given by

$$Q = \frac{2}{\pi^4}\delta^{-6} + \frac{3}{\pi^2}\delta^{-4} - \pi^2, \qquad R_c = \frac{2}{\pi^2}\delta^{-6} + 6\delta^{-4} + 6\pi^2\delta^{-2} + 2\pi^4. \quad (10)$$

We also scale the Prandtl number $\sigma = \delta^n \sigma_s$, where the exponent n of the scaling will be chosen below. The temperature field θ can be separated into its horizontal average T and the smaller horizontally varying component:

$$\theta(x, z) = T(z) + \delta\theta'(x, z), \quad (11)$$

where $\overline{\theta'}$ (the horizontal average of θ') is zero. For reflection-symmetric rolls, we also have $\overline{\Psi} = 0$. The PDEs for Ψ, T and θ' are then:

$$\delta^{3-n}(\Psi_z \Psi_{xxx} - \Psi_x \Psi_{xxz}) = \sigma_s \left(\frac{2}{\pi^4}\Psi_{zz} - \frac{2}{\pi^2} r\theta'_x\right), \quad (12)$$

$$\overline{\Psi_x \theta'_z} - \overline{\Psi_z \theta'_x} = T_{zz}, \quad (13)$$

$$\Psi_x T_z = \theta'_{xx} + \Psi_x, \quad (14)$$

where the subscripts x and z denote partial derivatives and we have kept only the leading order terms. Note that in the momentum equation (12), the exponent of the Prandtl number scaling has not yet been chosen, so the relative scaling of the nonlinear terms on the left and the buoyancy and Lorentz force terms on the right is undetermined at this stage. We remark that in this scaling the solution is not assumed to be small: Ψ is O(1).

The usual next step is to note that if the Prandtl number is large enough that the nonlinear terms in (12) can be dropped ($n < 3$), then the remaining leading-order equations are separable. Writing

$$\Psi(x, z) = \Psi_1(z)\sin x, \qquad \theta'(x, z) = \theta_1(z)\cos x, \quad (15)$$

we obtain three ODEs in z for Ψ_1, T and θ_1:

$$0 = \Psi_{1zz} + \pi^2 r\theta_1 \tag{16}$$

$$\frac{1}{2}\left(\Psi_1\theta_{1z} + \Psi_{1z}\theta_1\right) = T_{zz}, \tag{17}$$

$$\Psi_1 T_z = -\theta_1 + \Psi_1. \tag{18}$$

Even if $n \geqslant 3$, the leading-order nonlinear term in the momentum equation cancels exactly, providing Ψ contains only one horizontal wavenumber, and the same three ODEs are recovered. The equation for T_{zz} can be integrated to give

$$T_z = \frac{1}{2}\Psi_1\theta_1 + 1 - N, \tag{19}$$

where the integration constant $1 - N$ is the heat flux carried by convection between the lower and upper boundaries, and so N is the Nusselt number, a dimensionless measure of the total heat flux through the layer ($N = 1$ in the absence of convection). The other two equations are readily solved to give

$$\theta_1 = \frac{N\Psi_1}{1 + \frac{1}{2}{\Psi_1}^2} \tag{20}$$

and

$$\left(1 + \frac{1}{2}{\Psi_1}^2\right)\Psi_{1zz} + N\pi^2 r\Psi_1 = 0. \tag{21}$$

As this is a second-order boundary value problem for $\Psi(z)$, only the impermeability boundary conditions ($\Psi_1 = 0$ at $z = 0, 1$) can be applied. With this boundary condition, (21) gives $\Psi_{1zz} = 0$ at $z = 0, 1$, which implies that the temperature boundary condition $\theta_1 = 0$ is also satisfied through equation (16). Finally, integrating equation (19) introduces a second constant of integration that can be used to satisfy $T = 0$ at $z = 0, 1$. The resulting equation can be written as

$$1 - N\int_0^1 \frac{1}{1 + \frac{1}{2}{\Psi_1}^2}\,\mathrm{d}z = 0, \tag{22}$$

so the constant of integration N could be eliminated from (21) if required, resulting in an integro-differential equation. Note that the no-slip ($\Psi_{1z} = 0$) boundary condition cannot be applied at this order.

The same equation has been found by Matthews (1999) and Julien & Knobloch (1999). For given values of $r > 1$, equation (21) can be solved to find N and Ψ_1. An approximate truncated solution for r close to 1 can be readily computed:

$$\Psi_1 \approx \sqrt{8(r-1)}\sin\pi z, \tag{23}$$

with $N \approx 2r - 1$. For no-slip boundaries a more involved calculation involving viscous boundary layers shows that imposing the no-slip boundary condition $\Psi_{1z} = 0$ results in an $\mathrm{O}(\delta^3)$ correction that can be ignored at leading order. Matthews (1999) has also shown that for large (but not too large) values of r, the maximum value of Ψ_1 goes as $r\sqrt{\log r}$.

In principle, this approach can be carried on to higher order in δ, including more

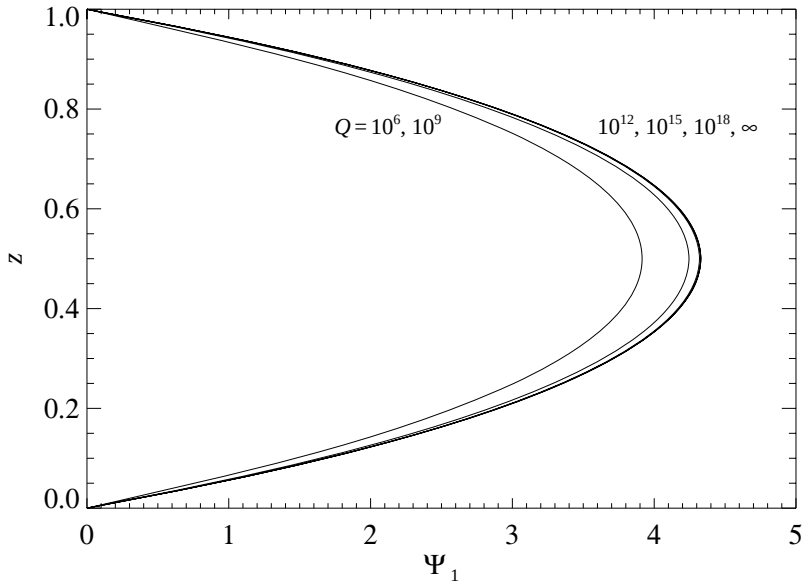

FIGURE 1. Nonlinear solutions of the full PDEs (6–7) with $Q = 10^6$, 10^9, 10^{12}, 10^{15} and 10^{18}, with the solution of the $Q = \infty$ asymptotic boundary value problem (21) overlaid. These solutions are for stress-free boundary conditions, $r = 2$ and have Prandtl numbers given in table 1. The maximum value of Ψ_1 (for $Q = \infty$) is $\Psi_{\rm mid} = 4.329449$, and the corresponding Nusselt number is $N = 3.67376$.

horizontal wavenumbers. However, if the Prandtl number is small ($n \geqslant 3$), attempting to go to higher order quickly leads to difficulties. If $n = 4$, for example, the largest term in the momentum equation (12) is the nonlinear term $\Psi_z \Psi_{xxx} - \Psi_x \Psi_{xxz}$ at order δ^{-1}. This term is zero when Ψ contains only one horizontal wavenumber (for example, $\sin x$), but any nonlinear solution will have components at all horizontal wavenumbers ($\sin 2x$, $\sin 3x$ and so on). We are working with an order one solution, so the amplitude of the $\sin x$ component is not small, but if the amplitudes of the higher wavenumber modes are of order δ, at order δ^{-1} in (12) there is still perfect cancellation. However, the order one part of (12) will now have contributions at all wavenumbers from the nonlinear part, forcing order one components in Ψ at all wavenumbers: a contradiction. One way of resolving this is if the higher-order wavenumbers have amplitudes smaller than order δ. A much more careful (numerical and analytic) investigation with $n = 4$ reveals that the next-order corrections to Ψ are of the form $\delta^3 \Psi_2(z) \sin(2x)$, and so on, but, in spite of this, it is not possible to construct a rational asymptotic approximation to the solution without introducing an arbitrary truncation in wavenumber.

Before proceeding to the stability calculations, we present in figure 1 numerical solutions of the full PDEs (6–7) with $Q = 10^6$, 10^9, 10^{12}, 10^{15} and 10^{18}, and $k = k_c$, with the solution of the $Q = \infty$ asymptotic boundary value problem (21) overlaid. The solutions and the asymptotic results are indistinguishable for $Q \geqslant 10^{12}$. These results are for Rayleigh numbers twice critical and for small Prandtl number, as given in table 1. (The

form of the solution scarcely changes as r decreases from 2 to unity, and the value 2 is adopted for illustration. The results of Busse & Clever (1996) suggest that smaller values than this should be chosen to ensure stability to knot-type modes in three dimensions.)

3.2. *Stability of convection in narrow rolls: leading order*

We next address the leading-order stability problem, considering only two-dimensional perturbations that preserve the horizontal periodicity, and that include a horizontal mean flow. It will turn out that the simplification we adopted above (truncation to one horizontal wavenumber) does not give a full description of the stability problem. However, to make analytic progress, we must adopt this simplification.

Supposing that we have already solved the nonlinear equation (21) to find steady fully nonlinear convection rolls, we now add a perturbation to the basic solution:

$$\Psi(x,z) = \Psi_1(z)\sin x + (\delta P_0(z) + P_1(z)\cos x)\, e^{st} \tag{24}$$

$$\theta(x,z) = T(z) + \delta\theta_1(z)\cos x + \delta Y_1(z)\sin x e^{st}, \tag{25}$$

where s is the growth rate of the instability, and $P_0(z)$, $P_1(z)$ and $Y_1(z)$ are all infinitesimal: products of these functions will be dropped. This is similar to the truncation used by Howard & Krishnamurti (1986). We set $s = 0$ for a steady-state instability, and substitute the above into the governing PDEs, retaining only the horizontal average and the first wavenumber component. This yields the ODEs

$$\begin{aligned} U_0\Psi_1\cos x + \delta\frac{1}{2}\frac{\mathrm{d}}{\mathrm{d}z}\left(P_1\Psi_{1zz} - P_{1zz}\Psi_1\right) + \mathrm{O}(\delta^2) \\ = \sigma_s\delta^{n-4}\left(-\frac{2r}{\pi^2}Y_1\cos x + \frac{2}{\pi^4}P_{1zz}\cos x - \delta\frac{2}{\pi^4}U_{0z} + \mathrm{O}(\delta^2)\right), \end{aligned} \tag{26}$$

$$P_1 T_z = Y_1 + P_1 + \mathrm{O}(\delta^2), \tag{27}$$

where U_0 is the (scaled) mean horizontal velocity: $U_0 = -P_{0z}$.

The right-hand side of (26), which has contributions only from the buoyancy and Lorentz forces at this order, is balanced with the advection terms on the left-hand side when $n = 4$, that is, when the Prandtl number σ scales as k^{-4} (or as $Q^{-2/3}$). For this value of n, the above equations are solved for the mean flow

$$U_0 = \frac{\pi^4}{4\sigma_s}\left(P_{1zz}\Psi_1 - P_1\Psi_{1zz}\right), \tag{28}$$

where the constant of integration is zero so that there is no net horizontal momentum averaged over the layer. The heat equation is rearranged to give

$$Y_1 = P_1(T_z - 1) = P_1\left(\frac{1}{2}\Psi_1\theta_1 - N\right) = -\frac{NP_1}{1 + \frac{1}{2}{\Psi_1}^2}. \tag{29}$$

These two expressions are then substituted into the fluctuating part of the momentum equation:

$$\frac{\pi^4}{4\sigma_s}\left(P_{1zz}\Psi_1 - P_1\Psi_{1zz}\right)\Psi_1 = \frac{2\sigma_s}{\pi^4}\left(\frac{N\pi^2 r P_1}{1 + \frac{1}{2}{\Psi_1}^2} + P_{1zz}\right) \tag{30}$$

yielding, after using (21) to substitute for Ψ_{1zz}, an ODE for P_1:

$$\left(\frac{\pi^8}{8\sigma_s^2}{\Psi_1}^2 - 1\right) \times \left(\left(1 + \frac{1}{2}{\Psi_1}^2\right) P_{1zz} + N\pi^2 r P_1\right) = 0. \tag{31}$$

The boundary conditions are $P_1 = 0$ at $z = 0$, 1.

In principle, we would expect to fix the Rayleigh number r, solve (21) for Ψ_1 and N, and then find that (31) has non-zero solutions only for certain values of the parameter σ_s. However, the first factor in (31) is non-zero for all values of z if $\sigma_s > \pi^4 \max|\Psi_1|/2\sqrt{2}$, and even if σ_s is smaller than this value, the first factor is non-zero for almost all values of z, and so can be cancelled. The remaining equation for P_1 has the unique solution $P_1 = \Psi_1$ (and $U_0 = 0$) for all values of σ_s. This corresponds to the neutrally stable translation mode of the original rolls, and is not an instability.

Thus there is no instability if we cancel the prefactor in (31), and the only possible instability must be associated with zeroes of this prefactor. Therefore, the only conclusion we can make at this order is that the Prandtl number must be small – less than $\delta^4\pi^4 2^{-3/2} \max|\Psi_1| = \pi^{\frac{4}{3}} 2^{-\frac{5}{6}} Q^{-2/3} \max|\Psi_1|$ – for a mean flow instability to take place, and that we would expect the instability to be concentrated close to where the prefactor changes sign. The situation resembles that which holds for critical layers in stratified shear flows – but the way in which the singularity at the critical layer is resolved (by means of thermal diffusion) is quite different in this case and so no direct comparison is possible.

3.3. *Higher order corrections*

Apart from the conclusion about the necessary order of magnitude of the Prandtl number, there is not enough information in the leading order equation for the perturbation (31) to determine the stability of the roll solution. One might think that the way to resolve this difficulty is to compute the next-order corrections to (31), which will prevent the prefactor $(\pi^8/8\sigma_s^2){\Psi_1}^2 - 1$ from cancelling. Unfortunately, before this can be done, the next-order correction to the basic state is also required, and consistency would demand including more horizontal wavenumbers. This is an unpleasant and unrevealing calculation (we have done it), and computing the correction to the perturbation is even worse – but there is an alternative.

The instability can only take place if the prefactor in (31) changes sign. The z-dependent part of this has a quadratic maximum at the midpoint of the layer (see figure 1), and we expect the eigenfunction to be concentrated near the midpoint, with a characteristic length scale related to the distance between the zero crossings. Since these will be close together for Prandtl numbers just below the value that allows the prefactor to change sign, we expect z derivatives in the eigenfunction to be enhanced, and the most important term in the correction to (31) to be the one with the most z derivatives. Unfortunately, we do not know what this term is, but the term with the most z derivatives in the correction to (21) is proportional to $\delta^2\Psi_{1zzzz}$.

We therefore suppose that when the next-order corrections are calculated, the resulting

equation is of the form:

$$\left(\frac{\pi^8}{8\sigma_s^2}{\Psi_1}^2-1\right)\times\left(\left(1+\frac{1}{2}{\Psi_1}^2\right)P_{1zz}+N\pi^2rP_1\right)=-\delta^2CP_{1zzzz} \tag{32}$$

plus δ^2 times lower derivatives in P_1, for some constant C. The minus sign on the right hand side is for later convenience. This is enough to allow some analytic progress to be made, with the proviso that the correction must be more complicated than the supposed $-\delta^2CP_{1zzzz}$, since we know that $P_1=\Psi_1$ must be a solution of (32) for all σ_s. Leaving this issue aside, the goal is to seek the value of σ_s as a function of δ (and therefore of Q) at which an instability takes place, so we treat (32) as an eigenvalue problem.

The next step is to expand about the point where the prefactor vanishes: $z=\frac{1}{2}$ and $\sigma_s=\pi^4\max|\Psi_1|/2\sqrt{2}$, with an appropriate scaling. Let $\Psi_{\rm mid}=\max|\Psi_1|=\Psi_1(\frac{1}{2})$ and $\Psi_{zz:\rm mid}=\Psi_{1zz}(\frac{1}{2})$, so that $\Psi_1\approx\Psi_{\rm mid}+\frac{1}{2}(z-\frac{1}{2})^2\Psi_{zz:\rm mid}$. Also let $\xi=\delta^{-m/2}(z-\frac{1}{2})$ and $\sigma_s=\pi^4\Psi_{\rm mid}/2\sqrt{2}-\delta^m\Delta\sigma$, where $\Delta\sigma$ is the scaled difference between the critical Prandtl number at finite Q and the limiting critical value, and $m>0$ is a number to be chosen below. With the common scaling of z and $\Delta\sigma$, the first nonzero terms of the Taylor expansion of the prefactor are balanced:

$$\frac{\pi^8}{8\sigma_s^2}{\Psi_1}^2-1=\delta^m\left(\frac{4\sqrt{2}}{\pi^4\Psi_{\rm mid}}\Delta\sigma+\frac{\Psi_{zz:\rm mid}}{\Psi_{\rm mid}}\xi^2\right)+{\rm O}(\delta^{2m}). \tag{33}$$

Next, we write the z derivatives in the eigenfunction in terms of the new coordinate ξ: $P_{1zz}=\delta^{-m}P_{1\xi\xi}$ and $P_{1zzzz}=\delta^{-2m}P_{1\xi\xi\xi\xi}$, and rewrite (32), dropping the P_1 term as it is small compared with $P_{1\xi\xi}$, yielding at leading order:

$$\delta^m\left(\frac{4\sqrt{2}}{\pi^4\Psi_{\rm mid}}\Delta\sigma+\frac{\Psi_{zz:\rm mid}}{\Psi_{\rm mid}}\xi^2\right)\times\left(1+\frac{1}{2}{\Psi_{\rm mid}}^2\right)\delta^{-m}P_{1\xi\xi}=-\delta^{2-2m}CP_{1\xi\xi\xi\xi}. \tag{34}$$

We have replaced $1+\frac{1}{2}{\Psi_1}^2$ by its value at the midlayer. Choosing $m=1$ balances both sides of this equation, which implies z derivatives scaling as $\delta^{-\frac{1}{2}}\sim Q^{1/12}$. We write $W=P_{1\xi\xi}$ and define $A=4\sqrt{2}(1+\frac{1}{2}{\Psi_{\rm mid}}^2)/\pi^4\Psi_{\rm mid}$ and $B=-\Psi_{zz:\rm mid}(1+\frac{1}{2}{\Psi_{\rm mid}}^2)/\Psi_{\rm mid}$. Using (21), we can also write $B=N\pi^2r$. With these definitions, we have the equation:

$$CW_{\xi\xi}+\left(A\Delta\sigma-B\xi^2\right)W=0. \tag{35}$$

The boundary conditions are that $W\to0$ as $\xi\to\pm\infty$. Solutions of this equation can be written in terms of Hermite polynomials times a Gaussian, which yields a discrete set of eigenvalues $\Delta\sigma$. The first solution and the lowest eigenvalue are:

$$W=\exp\left(-\frac{1}{2}\sqrt{\frac{B}{C}}\xi^2\right)\qquad\text{and}\qquad\Delta\sigma=\frac{\sqrt{BC}}{A}, \tag{36}$$

since the first Hermite polynomial is just a constant. We have assumed here that C is positive; the definitions of A and B above ensure that these are positive. The resulting predictions for the leading order mean flow and the value of the critical Prandtl number

are

$$U_0(z) = \delta^{-1}\frac{\pi^4}{4\sigma_s}\exp\left(-\frac{1}{2}\sqrt{\frac{B}{C}}\frac{(z-\frac{1}{2})^2}{\delta}\right)\Psi_1(z) \tag{37}$$

and

$$\sigma = \delta^4\left(\frac{\pi^4\Psi_{\rm mid}}{2\sqrt{2}} - \delta\frac{\sqrt{BC}}{A}\right) = Q^{-2/3}\left(\frac{\pi^{4/3}\Psi_{\rm mid}}{2^{5/6}} - Q^{-1/6}\frac{2^{5/6}}{\pi^{10/3}}\frac{\sqrt{BC}}{A}\right), \tag{38}$$

where we have used the leading order relation between δ and Q: $Q = 2\delta^{-6}/\pi^4$. We recall from (24) the scaling of P_0 implies that the true velocity is a factor of δ smaller than the U_0 given in (37), and so is in fact of the same order as P_1.

The conclusion of this calculation, which is based on the *assumption* that the leading order correction is of the form used in (32), is as follows. For a given value of the Rayleigh number r, the nonlinear eigenvalue problem (21) can be solved for N and $\Psi_1(z)$. The constants A and B can then be calculated, and a prediction can be made using (38) for the Prandtl number below which the basic state is unstable to mean flows. The mean flow is concentrated near the centre of the layer in a narrow region whose width scales as $Q^{-1/12}$, and so we expect the results to be independent of the top and bottom boundary conditions. By choosing higher order Hermite polynomials, subsequent instabilities can also be found; in particular, the first eigenfunction above is even about the midlayer, and the second is odd. The relative difference between these two eigenvalues should also scale as $Q^{-1/6}$.

The only remaining fly in the ointment is the assumption we had to make: that the leading order correction to the perturbation equation is of the form $-\delta^2 C P_{1zzzz}$, with C an unknown coefficient. Nonetheless, we have a prediction for the scaling of the critical Prandtl number (which turns out below to be surprisingly good) and for the form of the mean flow (which is not so good).

Careful asymptotic investigation of the PDEs using the one-wavenumber truncation as in (24) reveals that the assumed form of the stability problem is indeed correct – for the truncated PDEs – and leads to an estimate for the unknown coefficient: $C = 1 + \frac{1}{2}{\Psi_{\rm mid}}^2 = 1 + 4\sigma_s^2/\pi^8$. This term comes from the next-order part of the nonlinear term in the momentum equation. A full treatment of the stability problem for the full PDEs would require including more wavenumbers, and would in any case have to be truncated (since all wavenumbers appear at the next order). There is little advantage in doing this over solving the PDEs numerically.

4. Numerical results

We have computed steady roll solutions of the PDEs (6–7) at a Rayleigh number twice critical ($r = 2$), with imposed magnetic field Q varying from 10^6 up to 10^{18}. For stress-free boundary conditions, we used the code of Rucklidge (1994), with up to 68×68 Fourier modes, which is only just enough to resolve the case $Q = 10^{18}$. For no-slip boundary conditions (up to $Q = 10^{15}$), we used the code of Prat, Mercader & Knobloch (1998),

Q	k	$\sigma Q^{2/3}$	$\max\lvert\Psi_1\rvert$	N	$Q^{1/6}\left(11.17998-\sigma Q^{2/3}\right)$
10^6	18.98	6.9232	3.914878	3.08493	42.6
10^9	60.39	10.0282	4.245571	3.55534	36.4
10^{12}	191.09	10.8744	4.319651	3.65990	30.6
10^{15}	604.31	11.09173	4.328449	3.67235	27.9
10^{18}	1911.00	11.15271	4.329347	3.67362	27.3
∞	∞	11.17998	4.329449	3.67376	—

TABLE 1. Solutions of the PDEs on the margin of the mean flow instability (with $r = 2$ and stress-free boundaries). The final line is the asymptotic result with $Q = \infty$, which is used to calculate $A = 0.139126$ and $B = 72.5171$, used in (35). The results for no-slip boundaries are almost identical, for example, with $Q = 10^9$, we find $k = 60.39$ and $\sigma Q^{2/3} = 10.0068$. The last column provides numerical verification that the deviation of $\sigma Q^{2/3}$ from its limiting value of 11.17998 scales as $Q^{-1/6}$.

with up to 24 Fourier modes in the horizontal and 112 Tchebychev functions in the vertical. We decreased the Prandtl number σ until we found an instability, computing the eigenvalues of the Jacobian matrix linearised about the steady roll solution. We also solved the nonlinear eigenvalue problem (21) using AUTO (Doedel *et al.* 1997) with 200 collocation points. The PDE roll solutions at finite Q are compared with the $Q = \infty$ asymptotic solution in figure 1.

In figure 2 we show the eigenfunctions $U_0(z)$ of the mean flow instability from the PDE calculations compared with the predictions made above. Details of the PDE results are in table 1, with the value of σ just below the critical value. The figure also shows eigenfunctions computed with no-slip boundary conditions, which are almost indistinguishable from the stress-free results for $Q \geqslant 10^{12}$. Clearly this is because the eigenfunction is concentrated towards the centre of the layer.

With $r = 2$, the solution of the nonlinear eigenvalue problem (21) for $Q = \infty$ has $\Psi_{\rm mid} = 4.329449$ and $N = 3.67376$, which results in values for the other parameters: $A = 0.139126$, $B = 72.5171$ and $\sigma_s = 149.1033$, and a limiting value of $\sigma Q^{2/3} = 11.17998$. From table 1, we estimate the asymptotic value of $Q^{1/6}\left(11.17998-\sigma Q^{2/3}\right)$ to be about 25 – the value of 27.3 for $Q = 10^{18}$ is slightly suspect because of being on the limit of the resolution of the code, and we have extrapolated the remaining numbers to $Q \to \infty$ assuming a further correction that scales as $Q^{-1/6}$. Figure 3 presents the data in the last column of table 1: the difference between $\pi^{4/3}2^{-5/6}\Psi_{\rm mid} = 11.17998$, which is the predicted value of $\sigma Q^{-2/3}$, and the actual value of $\sigma Q^{-2/3}$. The figure confirms that the difference scales as $Q^{-1/6}$, and the factor 25 required to position the solid scaling law line correctly leads to an estimate of the parameter $C = 108$, and hence to the width of

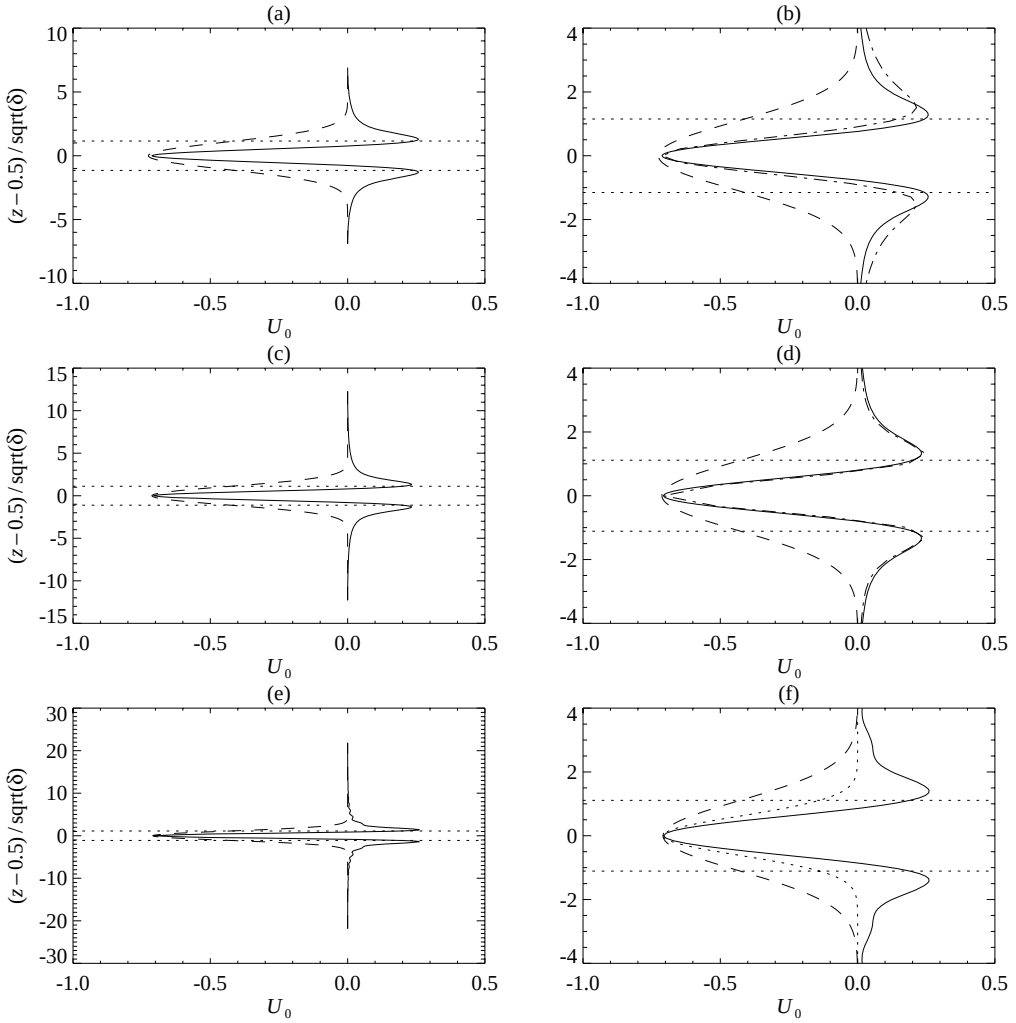

FIGURE 2. PDE solutions: eigenfunction of the mean flow instability, with stress-free boundary conditions. The mean flow, $U_0 = -P_{0z}$, is plotted as a function of ξ, the scaled depth. (a,b) $Q = 10^{12}$, $\sigma = 10.874 \times 10^{-8}$; (c,d) $Q = 10^{15}$, $\sigma = 11.0916 \times 10^{-10}$; (e,f) $Q = 10^{18}$, $\sigma = 11.1517 \times 10^{-12}$. Left column: the whole eigenfunction; right column: detail near the mid-layer. The eigenfunction is scaled so that P_{1zz} at $z = \frac{1}{2}$ is -1. The horizontal dotted lines indicate the positions where the prefactor in (31) changes sign. The dashed lines are Gaussians of the form $-\exp\left(-\sqrt{B/C}(z-\frac{1}{2})^2/2\delta\right)$, the prediction from (37). In (b) and (d), we have superposed (dash-dotted line) results with no-slip boundary conditions and (b) $\sigma = 10.87 \times 10^{-8}$; (d) $\sigma = 11.067 \times 10^{-10}$. In (f), we have superposed (dotted line) a Gaussian computed with $C = 1 + \frac{1}{2}{\Psi_{\rm mid}}^2$ instead of the value estimated from figure 3.

the predicted (from (36)) eigenfunctions in figure 2 (dashed Gaussian curves). The figure also confirms that no-slip boundaries do not affect the results.

As discussed in the previous section, assuming that the PDE is well represented by its truncation to a single wavenumber results in a different estimate for $C = 1 + \frac{1}{2}{\Psi_{\rm mid}}^2 = 10.372$. This is an order of magnitude smaller than the result obtained from the numerical

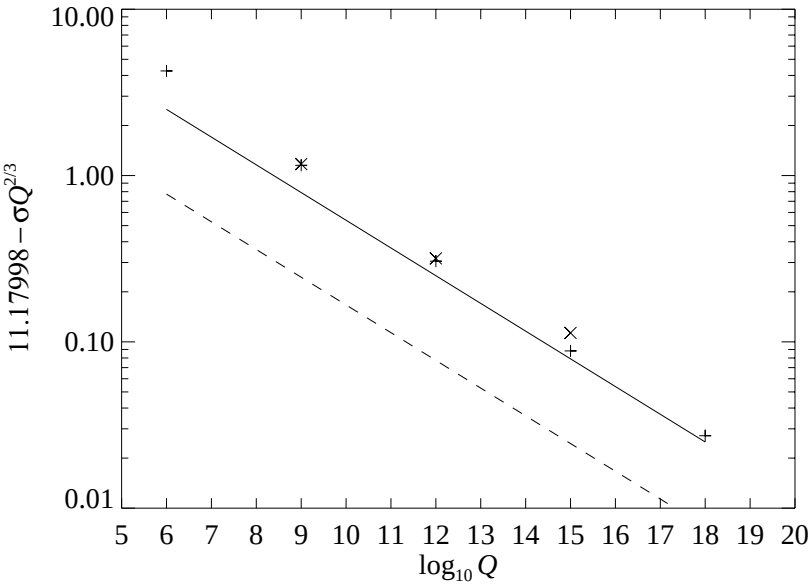

Figure 3. Discrepancy $\Delta\sigma$ as a function of Q between the Prandtl number and the value predicted for $Q = \infty$. Results with stress-free boundary conditions are shown as +; Results with no-slip boundary conditions are shown as ×. The solid line is the scaling law $25Q^{-1/6}$ – the coefficient in this scaling leads to an estimate for $C = 108$. Using $C = 1 + \frac{1}{2}{\Psi_{\rm mid}}^2 = 10.372$ instead yields the dashed line.

solutions of the PDEs above. The truncation also predicts that the eigenfunctions should be Hermite polyniomials times a Gaussian. Figure 2(f) shows a Gaussian (dotted) with this smaller value of C, and similarly, we plot the dashed line in figure 3. It is clear from figure 2 that neither value of C is correct – and that the eigenfunctions are not Gaussian – but in spite of this, the asymptotic value of the critical Prandtl number, and the correction to this value, scale as predicted.

5. Discussion

Clearly, the eigenfunctions in figure 2 are not simple Gaussians, but the overall width of the eigenfunctions scales correctly, when using the value of C obtained from figure 3. The appreciable size of the overshoot of the eigenfunction (horizontal velocity of opposite sign) is a consequence of overall conservation of momentum: the average value of U_0 is zero, since $U_0 = -P_{0z}$ and P_0 is zero at the top and bottom boundaries. The Gaussian predictions appear at first glance to have a net horizontal velocity, but it should be remembered that these are defined for $-\infty < \xi < \infty$, so an infinitesimal shift of the Gaussian will result in no net horizontal momentum. Nor does the eigenfunction correspond to a higher-order Hermite polynomial: the next even eigenfunction of (35) has positive and negative extrema that are equal in magnitude.

The reason, we believe, that the predicted results do not correspond in detail to the

actual results is that going to next order requires the inclusion of all horizontal wavenumbers, and the prediction relies on a truncation to a single horizontal wavenumber. In contrast, the leading order behaviour is genuinely described by a single horizontal wavenumber, owing to the exact cancellation of the nonlinear term in the momentum equation.

Taking the limit of narrow rolls has been a fruitful way of calculating fully nonlinear solutions of various convection situations: strong magnetic fields (or rapid rotation in other problems) leads to asymptotically narrow rolls where analytic progress can be made. In this paper, we have shown how the next step can be taken: calculating the stability of these fully nonlinear solutions. We have concentrated on mean flow instabilities that preserve the periodicity of the rolls, in the case of convection in a liquid metal with a strong imposed magnetic fields. Instability only occurs if the Prandtl number is smaller than $\pi^{4/3}2^{-5/6}\Psi_{\rm mid}Q^{-2/3}$, in the limit of large magnetic fields. This result comes out at leading order: the Prandtl number must be this small in order to allow the prefactor in (31) to change sign, and without this, there can be no instability. This leading order prediction does not require a solution of the eigenvalue problem.

In order to compute the form of the eigenfunction, it is necessary to carry the calculations to higher order, but bringing in correction terms means the solution no longer has a single horizontal wavenumber, and the advection term in the momentum equation brings in all horizontal wavenumbers. In order to make progress, we assumed a simple but plausible form for the correction to the linearised problem, which leads to a prediction for the scaling of the Prandtl number at which the instability occurs, and for the forms of the eigenfunction: the mean flow is concentrated in a jet of width $Q^{-1/12}$ in the middle of the layer. Because the eigenfunction has appreciable amplitude only close to the middle of the layer, the result applies to the cases of stress-free and no-slip top and bottom boundaries. Numerical solutions of the PDEs (for Q up to 10^{18}) indicate the correctness of the Prandtl number scaling, but the predicted Gaussian eigenfunctions are only in rough agreement with the actual eigenfunctions. Nonetheless, the mean flow is concentrated near the midpoint as predicted, and the width of the eigenfunction is at least in qualitative agreement.

The difficulty of the calculations mean that we have restricted ourselves to seeking only instabilities to steady flows, in a parameter regime relevant to liquid metals ($\zeta \gg 1$). Shear flow instabilities are known to occur in in a variety of situations, particularly when the Prandtl number is small (Howard & Krishnamurti 1986, Proctor *et al.* 1994, Rucklidge & Matthews 1996). Our asymptotic results are probably beyond the limit of what is achievable currently in the laboratory, though numerical results suggest that the instabilities will still occur for lower values for Q and correspondingly higher values of the Prandtl number σ. Moreover, we note that the critical Prandtl number increases with r.

This paper only addresses the linear instability to shear flows, but a sample timestepping calculation (figure 4) with $Q = 10^6$, $r = 2$ and $\sigma = 6.5 \times 10^{-4}$ (just below critical) leads to a steadily travelling wave with mean flow similar to that depicted in figure 2, showing that the bifurcation is supercritical. For smaller Prandtl number, we would ex-

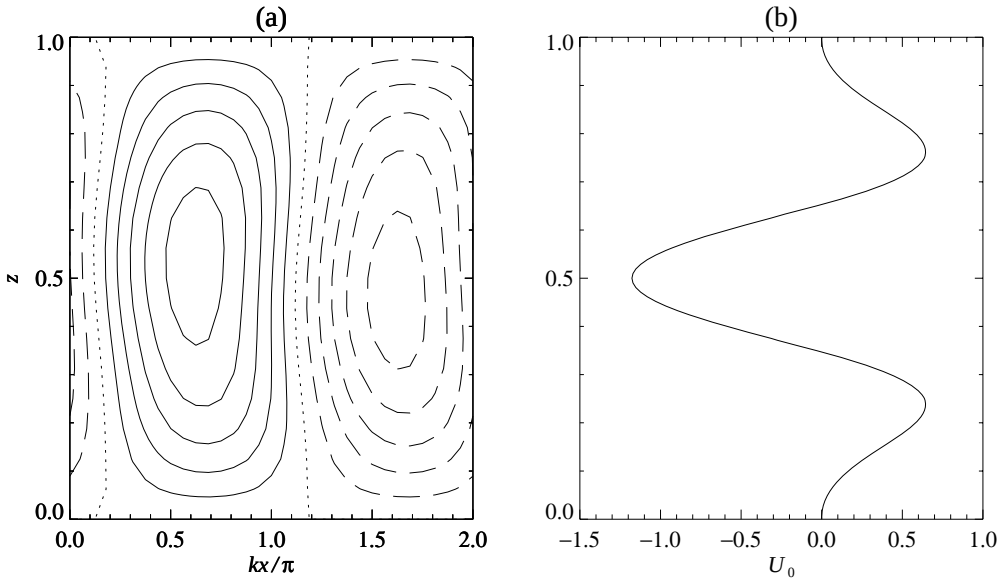

FIGURE 4. Fully nonlinear numerical solution of the PDE, with $Q = 10^6$, $r = 2$ and $\sigma = 6.5\times10^{-4}$ (just below critical), showing a steadily travelling wave. (a) Stream-function; (b) mean flow U_0 as a function of depth z – compare with figure 2.

pect to see tertiary instabilities and noise sensitive chaotic dynamics, as described by Hughes & Proctor (1990) and Rucklidge & Matthews (1996), and possibly instabilities to three-dimensional flows (Matthews *et al.* 1996).

We are grateful to Keith Julien for very useful discussions, and we thank David Hughes, Edgar Knobloch, Paul Matthews and Steve Tobias for helpful suggestions. JP is grateful for support from CIRIT (Catalonia) under grant BE94 from DGICYT (Spain) under grant PB94-1216. AMR is grateful for support from EPSRC. We also thank Père Magloire for inspiration at an early stage of this project.

REFERENCES

Abdulrahman, A., Jones, C.A., Proctor, M.R.E. and Julien, K., Large wavenumber convection in the rotating annulus. *Geophys. Astrophys. Fluid Dynamics*, 2000, **93**, 227–252.

Bassom, A.P. and Zhang, K., Strongly nonlinear convection cells in a rapidly rotating fluid layer. *Geophys. Astrophys. Fluid Dynamics*, 1994, **76**, 223–238.

Busse, F.H., Mean flow induced by a thermal wave. *J. Atmos. Sci.*, 1972, **29**, 1423–1429.

Busse, F.H., Generation of mean flows by thermal convection. *Physica*, 1983, **9D**, 287–299.

Busse, F.H. and Clever, R.M., An asymptotic model of two-dimensional convection in the limit of low Prandtl number. *J. Fluid Mech.*, 1981, **102**, 75–83.

Busse, F.H. and Clever, R.M., Three-dimensional convection in the presence of strong vertical magnetic fields. *Eur. J. Mech. B – Fluids*, 1996, **15**, 1–15.

Chandrasekhar, S., On the inhibition of convection by a magnetic field. *Phil. Mag.*, 1952, **43**, 501–532.

Chandrasekhar, S., *Hydrodynamic and Hydromagnetic Stability*, 1961 (Clarendon Press: Oxford).

Clune, T. and Knobloch, E., Pattern selection in three-dimensional magnetoconvection. *Physica*, 1994, **74D**, 151–176.

Dawes, J.H.P., Rapidly rotating thermal convection at low Prandtl number. *J. Fluid Mech.*, 2001, **428**, 61–80.

Doedel, E.J., Champneys, A.R., Fairgrieve, T.F., Kuznetsov, Y.A., Sandstede, B. and Wang, X. 1997 AUTO 97: Continuation and bifurcation software for ordinary differential equations (with HomCont).

Halford, A.R. and Proctor, M.R.E., An oscillatory secondary bifurcation for magnetoconvection and rotating convection at small aspect ratio. *J. Fluid Mech.*, 2002, **467**, 241–257.

Holyer, J.Y. and Proctor, M.R.E., Planform selection in salt fingers. *J. Fluid Mech.*, 1986, **168**, 241–253.

Howard, L.N. and Krishnamurti, R., Large-scale flow in turbulent convection: a mathematical model. *J. Fluid Mech.*, 1986, **170**, 385–410.

Hughes, D.W. and Proctor, M.R.E., A low-order model of the shear instability of convection: chaos and the effect of noise. *Nonlinearity*, 1990, **3**, 127–153.

Julien, K. and Knobloch, E., Fully nonlinear oscillatory convection in a rotating layer. *Phys. Fluids*, 1997, **9**, 1906–1913.

Julien, K. and Knobloch, E., Strongly nonlinear convection cells in a rapidly rotating fluid layer: the tilted f-plane. *J. Fluid Mech.*, 1998, **360**, 141–178.

Julien, K. and Knobloch, E., Fully nonlinear three-dimensional convection in a rapidly rotating layer. *Phys. Fluids*, 1999, **11**, 1469–1483.

Julien, K., Knobloch, E. and Tobias, S.M., Strongly nonlinear magnetoconvection in three dimensions. *Physica*, 1999, **128D**, 105–129.

Julien, K., Knobloch, E. and Tobias, S.M., Nonlinear magnetoconvection in the presence of strong oblique fields. *J. Fluid Mech.*, 2000, **410**, 285–322.

Matthews, P.C., Asymptotic solutions for nonlinear magnetoconvection. *J. Fluid Mech.*, 1999, **387**, 397–409.

Matthews, P.C., Proctor, M.R.E., Rucklidge, A.M. and Weiss, N.O., Pulsating waves in nonlinear magnetoconvection. *Phys. Lett. A*, 1993, **183**, 69–75.

Matthews, P.C., Rucklidge, A.M., Weiss, N.O. and Proctor, M.R.E., The three-dimensional development of the shearing instability of convection. *Phys. Fluids*, 1996, **8**, 1350–1352.

Prat, J., Massaguer, J.M. and Mercader, I., Large-scale flows and resonances in 2-D thermal convection. *Phys. Fluids*, 1995, **7**, 121–134.

Prat, J., Mercader, I. and Knobloch, E., Resonant mode interaction in Rayleigh–Bénard convection. *Phys. Rev. E*, 1998, **58**, 3145–3156.

Proctor, M.R.E., Columnar convection in double-diffusive systems. *Contemp. Math.*, 1986, **56**, 267–276.

Proctor, M.R.E. 2004 Magnetoconvection. In *Fluid Dynamics in Astrophysics and Geophysics* (ed. A.M. Soward, C. Jones, D. Hughes and N. Weiss), pp. . Boca Raton, FL: CRC Press.

Proctor, M.R.E. and Weiss, N.O., Magnetoconvection. *Rep. Prog. Phys.*, 1982, **45**, 1317–1379.

Proctor, M.R.E., Weiss, N.O., Brownjohn, D.P. and Hurlburt, N.E., Nonlinear compressible magnetoconvection. Part 2. Streaming instabilities in two dimensions. *J. Fluid Mech.*, 1994, **280**, 227–253.

Rucklidge, A.M., Chaos in magnetoconvection. *Nonlinearity*, 1994, **7**, 1565–1591.

Rucklidge, A.M. and Matthews, P.C., Analysis of the shearing instability in nonlinear convection and magnetoconvection. *Nonlinearity*, 1996, **9**, 311–351.

Russell, C.L., Blennerhassett, P.J. and Stiles, P.J., Supercritical analysis of strongly nonlinear vortices in magnetized ferrofluids. *Proc. R. Soc. Lond.* A, 1999, **455**, 23–67.

Soward, A.M., Convection-driven dynamo 1. Weak field case. *Phil. Trans. R. Soc. Lond.* A, 1974, **275**, 611–646.

Thompson, W.B., Thermal convection in a magnetic field. *Phil. Mag.*, 1951, **42**, 1417–1432.

Willis, G E and Deardorff, J W, The oscillatory motions of Rayleigh convection. *J. Fluid Mech.*, 1970, **44**, 661–672.